

World Journal of *Gastrointestinal Oncology*

World J Gastrointest Oncol 2023 June 15; 15(6): 911-1104



REVIEW

- 911 Role of neoadjuvant therapy for nonmetastatic pancreatic cancer: Current evidence and future perspectives
Cassese G, Han HS, Yoon YS, Lee JS, Lee B, Cubisino A, Panaro F, Troisi RI
- 925 Pancreatic cancer, autoimmune or chronic pancreatitis, beyond tissue diagnosis: Collateral imaging and clinical characteristics may differentiate them
Tornel-Avelar AI, Velarde Ruiz-Velasco JA, Pelaez-Luna M

MINIREVIEWS

- 943 Vitamin E in the management of pancreatic cancer: A scoping review
Ekeuku SO, Etim EP, Pang KL, Chin KY, Mai CW
- 959 Paradigm shift of chemotherapy and systemic treatment for biliary tract cancer
Leowattana W, Leowattana T, Leowattana P
- 973 Analysis of load status and management strategies of main caregivers of patients with malignant tumors of digestive tract
Wang XY, Wang J, Zhang S
- 979 Emerging role of autophagy in colorectal cancer: Progress and prospects for clinical intervention
Ma TF, Fan YR, Zhao YH, Liu B

ORIGINAL ARTICLE**Basic Study**

- 988 Transcription factor glucocorticoid modulatory element-binding protein 1 promotes hepatocellular carcinoma progression by activating Yes-associate protein 1
Chen C, Lin HG, Yao Z, Jiang YL, Yu HJ, Fang J, Li WN
- 1005 5'tiRNA-Pro-TGG, a novel tRNA halve, promotes oncogenesis in sessile serrated lesions and serrated pathway of colorectal cancer
Wang XY, Zhou YJ, Chen HY, Chen JN, Chen SS, Chen HM, Li XB

Clinical and Translational Research

- 1019 Comprehensive analysis of distal-less homeobox family gene expression in colon cancer
Chen YC, Li DB, Wang DL, Peng H

Retrospective Cohort Study

- 1036 Development of a model based on the age-adjusted Charlson comorbidity index to predict survival for resected perihilar cholangiocarcinoma

Pan Y, Liu ZP, Dai HS, Chen WY, Luo Y, Wang YZ, Gao SY, Wang ZR, Dong JL, Liu YH, Yin XY, Liu XC, Fan HN, Bai J, Jiang Y, Cheng JJ, Zhang YQ, Chen ZY

Retrospective Study

- 1051 Diagnostic accuracy of apparent diffusion coefficient to differentiate intrapancreatic accessory spleen from pancreatic neuroendocrine tumors

Ren S, Guo K, Li Y, Cao YY, Wang ZQ, Tian Y

- 1062 Chicken skin mucosa surrounding small colorectal cancer could be an endoscopic predictive marker of submucosal invasion

Zhang YJ, Wen W, Li F, Jian Y, Zhang CM, Yuan MX, Yang Y, Chen FL

- 1073 Relationship between multi-slice computed tomography features and pathological risk stratification assessment in gastric gastrointestinal stromal tumors

Wang TT, Liu WW, Liu XH, Gao RJ, Zhu CY, Wang Q, Zhao LP, Fan XM, Li J

Observational Study

- 1086 Diagnostic value of circular free DNA for colorectal cancer detection

Cui Y, Zhang LJ, Li J, Xu YJ, Liu MY

CASE REPORT

- 1096 Advanced gastric cancer achieving major pathologic regression after chemoimmunotherapy combined with hypofractionated radiotherapy: A case report

Zhou ML, Xu RN, Tan C, Zhang Z, Wan JF

ABOUT COVER

Editorial Board of *World Journal of Gastrointestinal Oncology*, Rossana Berardi, MD, PhD, Director, Full Professor, Medical Oncology, Università Politecnica delle Marche, Ancona 60126, Italy. r.berardi@univpm.it

AIMS AND SCOPE

The primary aim of *World Journal of Gastrointestinal Oncology (WJGO, World J Gastrointest Oncol)* is to provide scholars and readers from various fields of gastrointestinal oncology with a platform to publish high-quality basic and clinical research articles and communicate their research findings online.

WJGO mainly publishes articles reporting research results and findings obtained in the field of gastrointestinal oncology and covering a wide range of topics including liver cell adenoma, gastric neoplasms, appendiceal neoplasms, biliary tract neoplasms, hepatocellular carcinoma, pancreatic carcinoma, cecal neoplasms, colonic neoplasms, colorectal neoplasms, duodenal neoplasms, esophageal neoplasms, gallbladder neoplasms, *etc.*

INDEXING/ABSTRACTING

The *WJGO* is now abstracted and indexed in PubMed, PubMed Central, Science Citation Index Expanded (SCIE, also known as SciSearch®), Journal Citation Reports/Science Edition, Scopus, Reference Citation Analysis, China National Knowledge Infrastructure, China Science and Technology Journal Database, and Superstar Journals Database. The 2022 edition of Journal Citation Reports® cites the 2021 impact factor (IF) for *WJGO* as 3.404; IF without journal self cites: 3.357; 5-year IF: 3.250; Journal Citation Indicator: 0.53; Ranking: 162 among 245 journals in oncology; Quartile category: Q3; Ranking: 59 among 93 journals in gastroenterology and hepatology; and Quartile category: Q3. The *WJGO*'s CiteScore for 2021 is 3.6 and Scopus CiteScore rank 2021: Gastroenterology is 72/149; Oncology is 203/360.

RESPONSIBLE EDITORS FOR THIS ISSUE

Production Editor: *Xiang-Di Zhang*; Production Department Director: *Xiang Li*; Editorial Office Director: *Jia-Ru Fan*.

NAME OF JOURNAL

World Journal of Gastrointestinal Oncology

ISSN

ISSN 1948-5204 (online)

LAUNCH DATE

February 15, 2009

FREQUENCY

Monthly

EDITORS-IN-CHIEF

Monjur Ahmed, Florin Burada

EDITORIAL BOARD MEMBERS

<https://www.wjgnet.com/1948-5204/editorialboard.htm>

PUBLICATION DATE

June 15, 2023

COPYRIGHT

© 2023 Baishideng Publishing Group Inc

INSTRUCTIONS TO AUTHORS

<https://www.wjgnet.com/bpg/gerinfo/204>

GUIDELINES FOR ETHICS DOCUMENTS

<https://www.wjgnet.com/bpg/GerInfo/287>

GUIDELINES FOR NON-NATIVE SPEAKERS OF ENGLISH

<https://www.wjgnet.com/bpg/gerinfo/240>

PUBLICATION ETHICS

<https://www.wjgnet.com/bpg/GerInfo/288>

PUBLICATION MISCONDUCT

<https://www.wjgnet.com/bpg/gerinfo/208>

ARTICLE PROCESSING CHARGE

<https://www.wjgnet.com/bpg/gerinfo/242>

STEPS FOR SUBMITTING MANUSCRIPTS

<https://www.wjgnet.com/bpg/GerInfo/239>

ONLINE SUBMISSION

<https://www.f6publishing.com>



Retrospective Study

Diagnostic accuracy of apparent diffusion coefficient to differentiate intrapancreatic accessory spleen from pancreatic neuroendocrine tumors

Shuai Ren, Kai Guo, Yuan Li, Ying-Ying Cao, Zhong-Qiu Wang, Ying Tian

Specialty type: Oncology

Provenance and peer review:

Unsolicited article; Externally peer reviewed.

Peer-review model: Single blind

Peer-review report's scientific quality classification

Grade A (Excellent): 0
Grade B (Very good): B
Grade C (Good): C
Grade D (Fair): 0
Grade E (Poor): 0

P-Reviewer: Gokce E, Turkey;
Uhlmann D, Germany

Received: December 30, 2022

Peer-review started: December 30, 2022

First decision: January 22, 2023

Revised: February 1, 2023

Accepted: April 19, 2023

Article in press: April 19, 2023

Published online: June 15, 2023



Shuai Ren, Kai Guo, Yuan Li, Ying-Ying Cao, Zhong-Qiu Wang, Ying Tian, Department of Radiology, Jiangsu Province Hospital of Chinese Medicine, Affiliated Hospital of Nanjing University of Chinese Medicine, Nanjing 210029, Jiangsu Province, China

Corresponding author: Zhong-Qiu Wang, MD, PhD, Chief Doctor, Department of Radiology, Jiangsu Province Hospital of Chinese Medicine, Affiliated Hospital of Nanjing University of Chinese Medicine, No. 155 Hanzhong Road, Nanjing 210029, Jiangsu Province, China.
zhongqiuwang0815@163.com

Abstract

BACKGROUND

Intrapancreatic accessory spleen (IPAS) shares similar imaging findings with hypervascular pancreatic neuroendocrine tumors (PNETs), which may lead to unnecessary surgery.

AIM

To investigate and compare the diagnostic performance of absolute apparent diffusion coefficient (ADC) and normalized ADC (lesion-to-spleen ADC ratios) in the differential diagnosis of IPAS from PNETs.

METHODS

A retrospective study consisting of 29 patients (16 PNET patients *vs* 13 IPAS patients) who underwent preoperative contrast-enhanced magnetic resonance imaging together with diffusion-weighted imaging/ADC maps between January 2017 and July 2020 was performed. Two independent reviewers measured ADC on all lesions and spleens, and normalized ADC was calculated for further analysis. The receiver operating characteristics analysis was carried out for evaluating the diagnostic performance of both absolute ADC and normalized ADC values in the differential diagnosis between IPAS and PNETs by clarifying sensitivity, specificity, and accuracy. Inter-reader reliability for the two methods was evaluated.

RESULTS

IPAS had a significantly lower absolute ADC ($0.931 \pm 0.773 \times 10^{-3} \text{ mm}^2/\text{s}$ *vs* $1.254 \pm 0.219 \times 10^{-3} \text{ mm}^2/\text{s}$) and normalized ADC value (1.154 ± 0.167 *vs* 1.591 ± 0.364) compared to PNET. A cutoff value of $1.046 \times 10^{-3} \text{ mm}^2/\text{s}$ for absolute ADC was

associated with 81.25% sensitivity, 100% specificity, and 89.66% accuracy with an area under the curve of 0.94 (95% confidence interval: 0.8536-1.000) for the differential diagnosis of IPAS from PNET. Similarly, a cutoff value of 1.342 for normalized ADC was associated with 81.25% sensitivity, 92.31% specificity, and 86.21% accuracy with an area under the curve of 0.91 (95% confidence interval: 0.8080-1.000) for the differential diagnosis of IPAS from PNET. Both methods showed excellent inter-reader reliability with intraclass correlation coefficients for absolute ADC and ADC ratio being 0.968 and 0.976, respectively.

CONCLUSION

Both absolute ADC and normalized ADC values can facilitate the differentiation between IPAS and PNET.

Key Words: Pancreas; Neuroendocrine tumors; Accessory spleen; Diffusion-weighted imaging; Diagnostic performance

©The Author(s) 2023. Published by Baishideng Publishing Group Inc. All rights reserved.

Core Tip: Intrapancreatic accessory spleen (IPAS) presents as a solitary, well-defined, hypervascular mass on contrast-enhanced computed tomography or contrast-enhanced magnetic resonance imaging. They are often misdiagnosed as small (< 3 cm) hypervascular pancreatic neuroendocrine tumors (PNETs). IPAS is innocuous in nature and does not require treatment. However, surgery and/or chemotherapy are recommended for PNETs. The overlap of imaging characteristics between IPAS and PNETs often requires surgical management. Therefore, preoperative characterization is of utmost importance. Our study demonstrated that both absolute apparent diffusion coefficient (ADC) and normalized ADC values (lesion-to-spleen ADC ratios) allow clinically relevant differentiation of IPAS from PNET.

Citation: Ren S, Guo K, Li Y, Cao YY, Wang ZQ, Tian Y. Diagnostic accuracy of apparent diffusion coefficient to differentiate intrapancreatic accessory spleen from pancreatic neuroendocrine tumors. *World J Gastrointest Oncol* 2023; 15(6): 1051-1061

URL: <https://www.wjgnet.com/1948-5204/full/v15/i6/1051.htm>

DOI: <https://dx.doi.org/10.4251/wjgo.v15.i6.1051>

INTRODUCTION

Ectopic splenic tissue, also known as an accessory spleen, is found in up to 30% of the population[1]. While accessory spleens are often observed at the splenic hilum, they can also be present in the pancreatic parenchyma[2]. Accessory spleens are usually of little clinical consequence and found incidentally during surgery for other indications. They can cause symptoms, most often hematologic, after a splenectomy has been carried out[3,4]. Intrapancreatic accessory spleen (IPAS) typically presents as a solitary, well-defined, hypervascular, ovoid or round mass with a maximum diameter < 3 cm on contrast-enhanced computed tomography (CE-CT) or magnetic resonance imaging (CE-MRI). They are often misdiagnosed as small (< 3 cm) hypervascular pancreatic neuroendocrine tumors (PNETs) since they share similar imaging findings[1,4-9]. IPAS is innocuous in nature and generally does not require any treatment. However, surgery and/or chemotherapy are recommended for PNETs[10]. Unfortunately, the overlap of imaging features between IPAS and small (< 3 cm) hypervascular PNETs often requires surgical management[11]. Therefore, preoperative characterization of IPAS *vs* small (< 3 cm) hypervascular PNETs is of utmost importance.

The investigation of diffusion-weighted imaging (DWI) in evaluating and characterizing pancreatic masses is increasing, with several studies clarifying its application in pancreatic tumor detection or the differentiation between benign and malignant pancreatic masses[12-14]. DWI is a method of signal contrast generation based on tissue cellularity, architecture, and cell membrane integrity, which can be quantified by apparent diffusion coefficient (ADC) maps. DWI can reflect the random microscopic motion of water molecules and provide information for tumor characterizing, staging, and differential diagnosis[12,14,15]. Recently, technical advancements have been achieved in decreasing imaging time and improving image quality. As a result, DWI is preferred and recommended since it allows non-invasive functional evaluation without the use of contrast media or ionizing radiation.

It has been shown that the splenic parenchyma possesses a markedly lower ADC value than the pancreatic parenchyma due to its unique organ composition. Obviously, significant differences with regard to ADC values have been observed between IPAS and PNETs since IPAS has similar tissue

structures and properties as the spleen[6]. However, concerns have been raised about inter- and intra-scanner ADC variability with contradicting results[16]. A recent study showed that though ADC measurements of the pancreas may be affected by the field strength of an MRI scanner, they demonstrate good reproducibility between different MR systems with the same field strength[17]. Notably, it has also been reported that ADC variability may be minimized by calculation of the normalized ADC value (lesion-to-spleen ADC ratios) with the assistance of technical factors in different organs and pathologies[18,19]. Therefore, the objective of our study was to investigate and compare the diagnostic accuracy of absolute ADC and normalized ADC values in differentiating IPAS from small (< 3 cm) hypervascular PNETs.

MATERIALS AND METHODS

Patients

This study was approved by our ethics committee with a waiver of informed consent due to its retrospective nature. We carried out a search of our radiology database of focal pancreatic masses to identify patients with IPAS and PNETs between January 2017 and July 2020. A total of 132 patients were identified from the database search (51 IPAS and 81 PNETs). Inclusion criteria for IPAS were as follows: (1) CE-MRI images together with DWI/ADC maps were available; (2) IPAS showed a purely solid lesion without cystic changes on MRI images; (3) Diagnosis of IPAS was made pathologically following surgical resection or endoscopic ultrasound-guided fine needle aspiration; and (4) IPAS cases without pathology or cytopathology were also included under the following criteria: the lesion was located at the tail of the pancreas and showed similar signal intensity/enhancement pattern compared with spleen; and the lesion remained stable in size (< 3 cm) and shape over at least 18 mo[1,6]. According to these criteria, 38 patients were excluded from the study, *i.e.* 34 patients did not have available CE-MRI or DWI/ADC, 1 patient had surgically-proven cystic changes within the lesion, and 3 patients were diagnosed based on imaging findings although the follow-up period was less than 18 mo. Finally, 13 patients with IPAS whose diagnosis was made by surgery ($n = 4$), biopsy ($n = 3$), and typical imaging findings ($n = 6$, follow-up period ≥ 18 mo) were included in this study (Figure 1).

Inclusion criteria for PNETs were as follows: (1) CE-MRI images together with DWI/ADC maps were available; (2) PNET showed a hypervascular purely solid mass without cystic changes on MRI images; (3) Diagnosis of PNET was made pathologically following surgical resection or endoscopic ultrasound-guided fine needle aspiration; and (4) PNET had a size < 3 cm without apparent distant metastasis on MRI images. According to these criteria, 65 patients were excluded from the study, *i.e.* 49 patients without available CE-MRI or DWI/ADC, 5 patients with hypovascular enhancement pattern or surgically-proven cystic changes within the lesion, 8 patients with a mass size > 3 cm, and 3 patients with metastasis. Finally, 16 patients with PNET whose diagnoses were made by surgery ($n = 11$) and biopsy ($n = 5$) were included into this study (Figure 1).

MRI protocol

A preoperative MRI scan was performed for all enrolled patients using a standard imaging protocol as described in our previous study[20]. A 3.0-T MRI system (Sigma HDx; GE Medical Systems, Milwaukee, WI, United States) with an eight-channel phased-array torso coil was adopted. DWI was obtained prior to contrast administration in all patients. DWI images with b values of 0, 50, and 1000 s/mm² were performed using a respiration-triggered single-shot echo-planar sequence. The imaging parameters were: a spectral pre-saturation with inversion recovery for fat suppression; repetition time, 8000 ms; echo time, 60 ms; slice thickness, 5 mm; interslice gap, 2 mm; flip angle 90°; matrix, 196 × 133; and field of view, 36 cm × 30 cm. In addition to DWI sequence, this study also adopted T1-weighted fat-suppressed liver acquisition with volume acceleration sequence (repetition time, 3100 ms; echo time, 15 ms; imaging duration, 60-120 s; slice thickness, 5 mm; interslice gap, 2 mm; flip angle, 12°; matrix, 384 × 256; and field of view, 22 cm × 22 cm) and fast spin-echo T2-weighted fat-suppressed sequence (repetition time, 6000 ms; echo time, 80 ms; imaging duration, 120-180 s; slice thickness, 5 mm; interslice gap, 2 mm; flip angle, 90°; matrix, 384 × 256; and field of view, 22 cm × 22 cm). T1-weighted contrast-enhanced images with triple phases including pancreatic parenchyma, portal venous, and delayed phases were obtained at 35 s, 70 s, and 240 s after bolus intravenous administration of gadopentetate dimeglumine (Bayer HealthCare Pharmaceuticals, Berlin, Germany) at a dose of 0.2 mmol/kg body weight followed by a 20-mL saline flush. The ADC values were calculated using a monoexponential function with b values of 0 and 1000 s/mm² due to the fact that high b-value DWI images contribute to better contrast, greater tissue diffusivity, and a lower T2 shine through effect[7].

Image analysis

One abdominal radiologist with 10 years of experience who was blinded to the final diagnosis performed all the ADC measurements of the lesions and spleens on ADC maps using circular or oval regions of interest (ROIs). ROIs of pancreatic lesions were placed to include maximum lesion areas, while the most peripheral portions were avoided to exclude volume averaging. The ROIs of the spleen

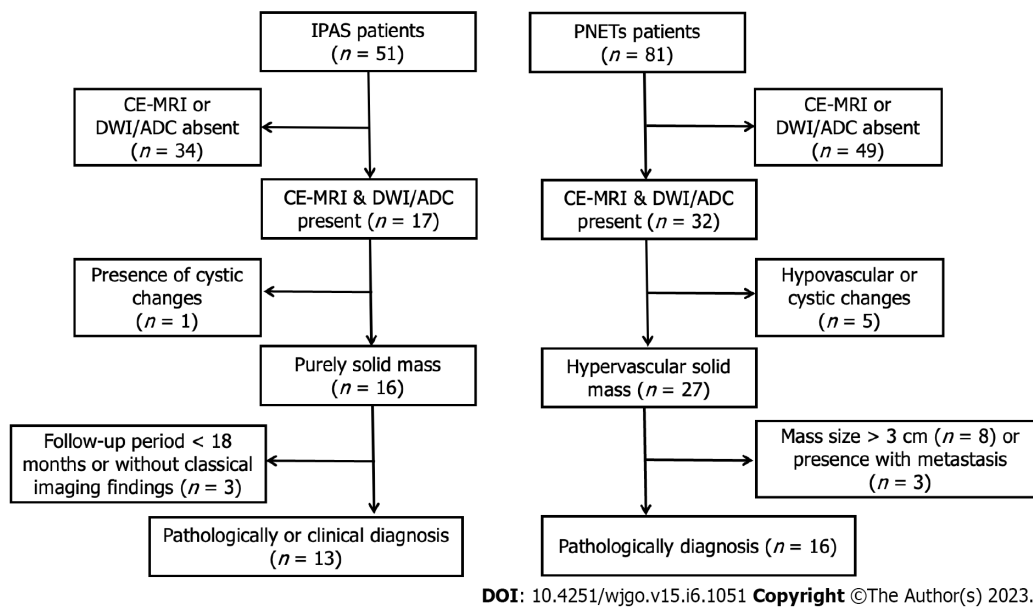


Figure 1 Flowchart of patients throughout the study. ADC: Apparent diffusion coefficient; CE-MRI: Contrast-enhanced magnetic resonance imaging; DWI: Diffusion-weighted imaging; IPAS: Intrapancreatic accessory spleen; PNETs: Pancreatic neuroendocrine tumors.

were placed on each of the anterior pole, mid pole, and posterior pole of the spleen with the purpose of avoiding volume averaging by excluding vessels and artifacts as much as possible. Finally, the average of the three splenic ADC measurements was adopted for the calculation of normalized ADC value (ADC of the pancreatic lesion/the average ADC of spleen).

Similar image analysis was carried out by a second abdominal radiologist (with 8 years of experience) with no prior knowledge of detailed histopathological information of any patients for inter-reader variability analysis. Quantitative data including absolute ADC and normalized ADC values from the reader with greater experience in abdominal MRI diagnosis was adopted for further analysis.

Statistical analysis

Statistical analysis was carried out using SPSS 20.0 and GraphPad Prism 8.0 software. The normal distribution and variance homogeneity of variables were analyzed by using the Kolmogorov-Smirnov test and Levene test, respectively. Normal distributed variables were described by mean \pm standard deviation (SD). The non-normal distributed variables were expressed as medians (first quartile, third quartile). The quantitative variables were compared by the two-tailed independent *t*-test or the Mann-Whitney *U* test. The receiver operating characteristics (ROC) analysis was carried out for evaluating the diagnostic performance of both absolute ADC and normalized ADC values in the differential diagnosis between IPAS and PNETs by clarifying sensitivity, specificity, and accuracy. The areas under the curves (AUCs) were determined for both absolute ADC and normalized ADC values, and the AUCs between these two methods were compared using the DeLong's test. Inter-reader reliability for both absolute ADC and normalized ADC values were assessed by using Bland-Altman analyses and intraclass correlation coefficient (ICC)[21]. ICC coefficients were defined as poor (< 0.40), fair ($0.40 \leq \text{ICC} < 0.60$), good ($0.60 \leq \text{ICC} < 0.75$), and excellent ($\text{ICC} \geq 0.75$). The statistical significance level was set at a *P* value < 0.05 .

RESULTS

Patient characteristics and imaging analysis

Twenty-nine patients including 16 PNET patients [10 males and 6 females; age range: 22-72 years; mean age: 52.38 years \pm 13.72 (SD)] and 13 IPAS patients [6 males and 7 females; age range: 27-78 years; mean age: 56.15 years \pm 15.78 (SD)] were finally included into the study. Among them, 16 PNET patients and 7 IPAS patients were diagnosed by pathology/cytopathology, while the remaining cases with IPAS were selected out based on typical imaging findings. No significant differences were found in sex or age between the two groups. All IPAS lesions were located at the tail of the pancreas. PNETs were located as follows: six tumors at the head and neck of the pancreas; and 7 at the body and tail of the pancreas.

MRI findings in patients with IPAS and PNET were shown in Table 1. No significant differences were found in lesion diameter, lesion ROI, or spleen ROI. Mean absolute ADC values for the spleen were not significantly different between the IPAS and PNET groups ($0.817 \pm 0.943 \times 10^{-3} \text{ mm}^2/\text{s}$ vs $0.806 \pm 0.145 \times$

Table 1 Magnetic resonance imaging findings in patients with intrapancreatic accessory spleen and small hypervascular pancreatic neuroendocrine tumors

Parameters	IPAS	PNETs	P value
Lesion diameter in mm	17.71 ± 5.09	18.21 ± 5.47	0.803
Lesion ROI in cm ²	0.685 ± 0.601	0.866 ± 0.567	0.413
Spleen ROI in cm ²	2.134 ± 0.805	2.753 ± 0.910	0.066
Spleen ADC as × 10 ⁻³ mm ² /s	0.817 ± 0.943	0.806 ± 0.145	0.825
aADC as × 10 ⁻³ mm ² /s	0.931 ± 0.773	1.254 ± 0.219	< 0.001
rADC	1.154 ± 0.167	1.591 ± 0.364	< 0.001

aADC: Absolute apparent diffusion coefficient; ADC: Apparent diffusion coefficient; IPAS: Intrapancreatic accessory spleen; PNETs: Pancreatic neuroendocrine tumors; rADC: Normalized apparent diffusion coefficient (lesion-to-spleen apparent diffusion coefficient ratios); ROI: Regions of interest.

10⁻³ mm²/s, $P = 0.825$). The absolute ADC and normalized ADC values were significantly different between IPAS and PNET (both $P < 0.001$), with IPAS showing lower absolute ADC values ($0.931 \pm 0.773 \times 10^{-3} \text{ mm}^2/\text{s}$ vs $1.254 \pm 0.219 \times 10^{-3} \text{ mm}^2/\text{s}$) and lower normalized ADC values (1.154 ± 0.167 vs 1.591 ± 0.364) compared to PNET. **Figure 2** shows two representative cases of IPAS and PNET. The absolute ADC and normalized ADC values of IPAS were significantly lower than those of PNET.

Diagnostic performance of ADC values

We subsequently evaluated the diagnostic performance of absolute ADC and normalized ADC values in differentiating IPAS from PNET. **Table 2** summarized the sensitivity, specificity, accuracy, positive predictive value, negative predictive value, and cutoff value of absolute ADC and normalized ADC values by ROC analysis. ROC analysis demonstrated the optimum cutoff value by maximizing the sum of sensitivity and specificity for differentiating IPAS from PNET. A cutoff value of $1.046 \times 10^{-3} \text{ mm}^2/\text{s}$ for absolute ADC was associated with 81.25% sensitivity, 100% specificity, and 89.66% accuracy with an AUC of 0.94 (95%CI: 0.8536-1.000) for the differential diagnosis of IPAS from PNET. Similarly, a cutoff value of 1.342 for normalized ADC was associated with 81.25% sensitivity, 92.31% specificity, and 86.21% accuracy with an AUC of 0.91 (95%CI: 0.8080-1.000) for the differential diagnosis of IPAS from PNET. **Figure 3** shows the ROC curves for absolute ADC and normalized ADC values. DeLong's test was used to compare the AUCs of two models established with absolute ADC and normalized ADC values in the differential diagnosis of IPAS from PNET. No statistically significant difference was found ($P = 0.6668$).

Inter-reader reliability analysis

The ICCs to evaluate inter-reader reliability for absolute ADC and normalized ADC values were 0.968 (95%CI: 0.933-0.985) and 0.976 (95%CI: 0.950-0.989), respectively. Bland-Altman analysis (**Figure 4**) revealed that the bias between two readers (solid blue line) was not significant for both absolute ADC and normalized ADC values, with the line of quality (dotted orange line) falling within the 95% CI of the mean difference (dotted blue lines).

DISCUSSION

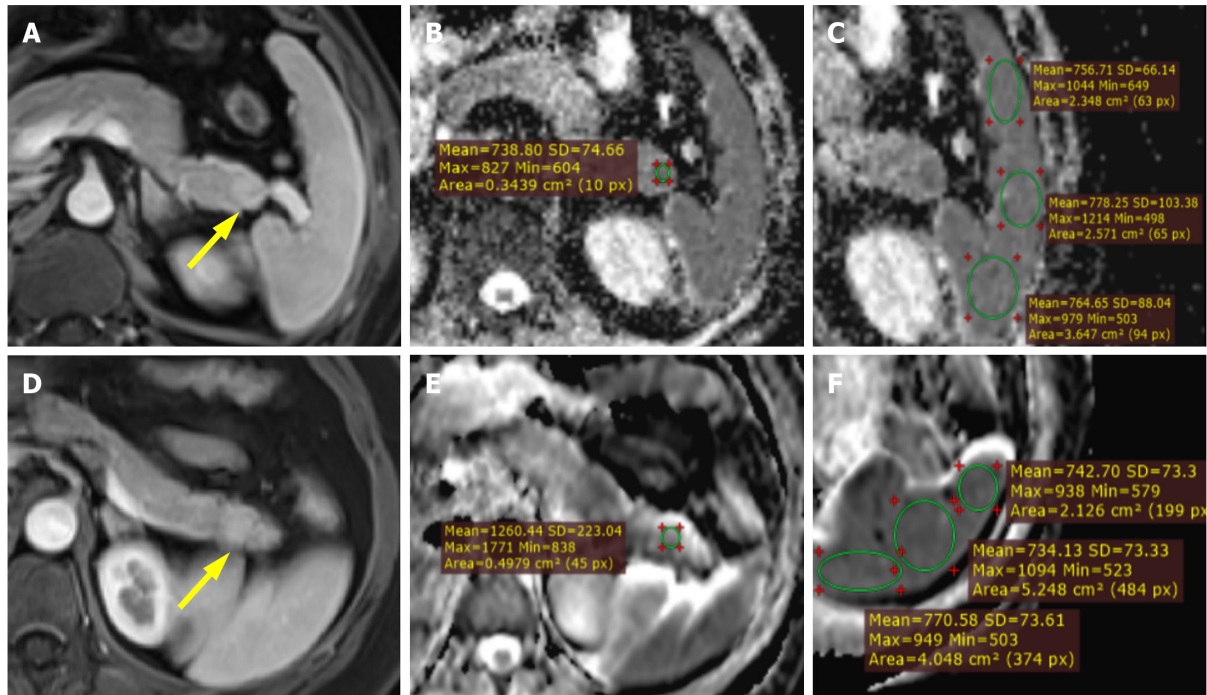
An IPAS is typically asymptomatic and has an innocuous nature, which does not require needle biopsy or surgery[11]. However, overlapping imaging features of IPAS and PNET may lead to unnecessary surgery. In many cases, despite imaging and other diagnostic studies, malignancy cannot be excluded, and patients are subjected to pancreatic resection. Therefore, there is a dire need to preoperatively characterize IPAS and differentiate them from PNET. Conventional MRI paved the way for differentiating IPAS from PNET in a non-invasive way since IPAS has similar tissue structure and properties as the spleen, which can be reflected by DWI, demonstrating that IPAS possesses a markedly lower ADC value than PNET[1,7]. In our current study, we found that absolute ADC and normalized ADC values can be used for the differential diagnosis between IPAS and PNET and showed a high pooled sensitivity and specificity.

Multiple modalities including contrast-enhanced ultrasound (CE-US), CT, superparamagnetic iron oxide-enhanced MRI, and nuclear medicine have been proven to be effective in discriminating IPAS from pancreatic solid tumors[5,8,22,23]. Among these, CE-US, ^{99m}Tc scintigraphy, and superparamagnetic iron oxide-enhanced MRI are performed with the intravenous administration of contrast media or the phagocytosis of nuclear pharmaceuticals by macrophages of the reticuloendothelial system

Table 2 Diagnostic performances of absolute apparent diffusion coefficient and normalized apparent diffusion coefficient values

Variables	AUC	Sensitivity, %	Specificity, %	PPV, %	NPV, %	Accuracy, %
aADC as $\times 10^{-3} \text{ mm}^2/\text{s}$	0.94	81.25	100	100	81.25	89.66
rADC	0.91	81.25	92.31	92.86	80.00	86.21

aADC: Absolute apparent diffusion coefficient; AUC: Area under curve; NPV: Negative predictive value; PPV: Positive predictive value; rADC: Normalized apparent diffusion coefficient (lesion-to-spleen apparent diffusion coefficient ratios).



DOI: 10.4251/wjgo.v15.i6.1051 Copyright ©The Author(s) 2023.

Figure 2 Magnetic resonance images. A-C: Magnetic resonance images in a 51-year-old male with pathologically proven intrapancreatic accessory spleen. The lesion was located at the tail of the pancreas with a hypervascular enhancement pattern on contrast-enhanced arterial phase T1 weighted imaging (T1WI) (yellow arrow, A). After confirming the lesion on arterial phase T1WI and diffusion-weighted imaging (B), circular regions of interest (ROI) were placed within the lesion on the apparent diffusion coefficient (ADC) map (B) and showed an ADC value of $0.738 \times 10^{-3} \text{ mm}^2/\text{s}$. Similarly, ADC measurement was carried out on the adjacent spleen using circular ROIs (C) and demonstrated an average splenic ADC of $0.767 \times 10^{-3} \text{ mm}^2/\text{s}$. The normalized ADC (lesion-to-spleen ADC ratio) was 0.962; D-F: Magnetic resonance images in a 45-year-old female with pathologically proven G2 pancreatic neuroendocrine tumor. The lesion was located at the tail of the pancreas with a hypervascular enhancement pattern on contrast-enhanced arterial phase T1WI (yellow arrow, D). After confirming the lesion on arterial phase T1WI and diffusion-weighted imaging (B), circular ROI was placed within the lesion on the ADC map (B) and showed an ADC value of $1.260 \times 10^{-3} \text{ mm}^2/\text{s}$. Similarly, ADC measurement was carried out on the adjacent spleen using circular ROIs (C) and demonstrated an average splenic ADC of $0.749 \times 10^{-3} \text{ mm}^2/\text{s}$. The normalized ADC (lesion-to-spleen ADC ratio) was 1.682.

in the spleen[7]. Although these modalities showed high pooled sensitivity and specificity, they have the following shortcomings: They rely on phagocytosis of macrophages, the application of which in splenic visualization is quite limited as it requires minimal functioning of splenic tissues; and contrast agents or exogenous nuclear pharmaceuticals[7]. In addition, scintigraphy has limited value when the pancreatic lesion has a relatively small size since it has lower spatial resolution compared with CT or MRI. In addition, CE-US has limited diagnostic utility in fully examining the pancreatic tail due to the limited sonic window and operator-independent nature[24]. In contrast, DWI does not require any exogenous contrast media or ionizing radiation and can be performed comparatively rapidly.

It has been reported that ADC variability may be minimized by calculation of the normalized ADC value (lesion-to-spleen ADC ratios) with the help of technical factors in different organs and pathologies [18,19]. In our study, we used absolute ADC and normalized ADC values to differentiate IPAS from PNET. The key findings of our study fall into two main categories: (1) Both absolute and normalized ADC values performed equally well in the discrimination of IPAS from PNET. A cutoff value of $1.046 \times 10^{-3} \text{ mm}^2/\text{s}$ for absolute ADC was associated with 81.25% sensitivity, 100% specificity, and 89.66% accuracy with an AUC of 0.94 (95%CI: 0.8536-1.000) for the differential diagnosis of IPAS from PNET. Similarly, a cutoff value of 1.342 for normalized ADC was associated with 81.25% sensitivity, 92.31%

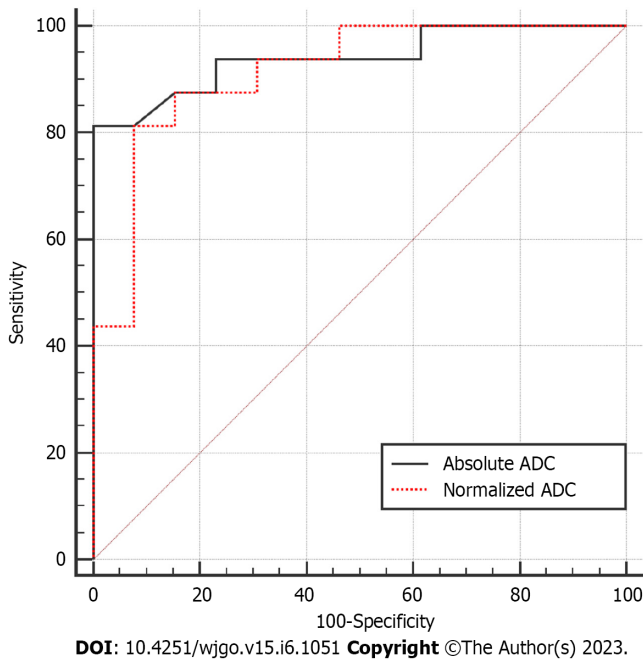


Figure 3 Receiver operating characteristic curve for diagnostic performance of absolute apparent diffusion coefficient and normalized apparent diffusion coefficient values regarding the differentiation between intrapancreatic accessory spleen and pancreatic neuroendocrine tumor. ADC: Apparent diffusion coefficient.

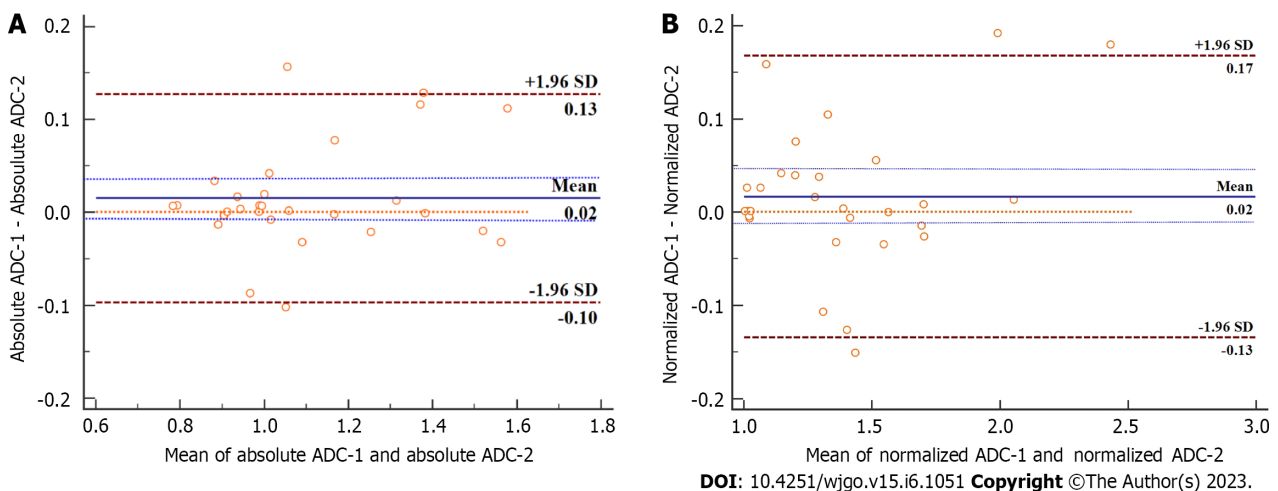


Figure 4 Bland-Altman plots of absolute apparent diffusion coefficient and normalized apparent diffusion coefficient for the two readers' measurements with the representation of the 95% limits of agreement (dotted and dashed brown lines). A: Absolute apparent diffusion coefficient (ADC); B: Normalized ADC. For both absolute ADC and normalized ADC values, the bias between two readers (solid blue line) was not significant, with the line of equality (dotted orange line) falling within the 95% confidence interval of the mean difference (dashed blue lines). SD: Standard deviation.

specificity, and 86.21% accuracy with an AUC of 0.91 (95%CI: 0.8080-1.000) for the differential diagnosis of IPAS from PNET; and (2) A high degree of inter-reader reliability for absolute ADC [0.968 (95%CI: 0.933-0.985)] and normalized ADC values [0.976 (95%CI: 0.950-0.989)] were obtained in our study. There was no significant difference in diagnostic performance between absolute ADC and normalized ADC values with high inter-reader reliability. In clinical practice, absolute ADC provides the ease of a single measurement. However, further studies with a larger cohort size may be necessary to evaluate the definite superiority of one method over the other.

The spleen has a much lower ADC compared to the pancreas since it has a unique organ composition. A previous study revealed that the mean ADC value of IPAS was significantly lower than that of PNET ($0.90 \times 10^{-3} \text{ mm}^2/\text{s}$ vs $1.44 \times 10^{-3} \text{ mm}^2/\text{s}$, $P < 0.001$); A cutoff value of $1.07 \times 10^{-3} \text{ mm}^2/\text{s}$ demonstrated high pooled sensitivity (96.0%) and specificity (93.5%) in the differential diagnosis between IPAS and PNET[6]. In our study, the absolute ADC and normalized ADC values of the IPAS were $0.931 \pm 0.773 \times 10^{-3} \text{ mm}^2/\text{s}$ and 1.154 ± 0.167 , respectively, which were significantly lower than those of PNETs ($1.254 \pm$

$0.219 \times 10^{-3} \text{ mm}^2/\text{s}$ and 1.591 ± 0.364). Our study was consistent with the previous study[6]. However, they did not investigate the potential value of the normalized ADC and their diagnostic performance in the differential diagnosis between the two entities. Our study showed an equal performance of both absolute ADC and normalized ADC values in the discrimination of IPAS from PNET and revealed a high degree of inter-reader reliability, which corroborated the findings a previous study demonstrated [1]. However, this study had unbalanced data with 51 PNETs and 11 IPAS lesions, and no algorithm was used to balance the data for further analysis.

Additionally, all patients underwent MRI scans using a 1.5-T MRI system, and a single scanner from one vendor was used to scan the patients. It is unclear whether the results can be generalized to all vendors. A recent study showed that ADC measurements of the pancreas may be affected by the field strength of the MRI scanner[17]. Our studies further validated that both absolute ADC and normalized ADC values are useful in the discrimination of IPAS from PNET with the 3.0-T MRI system and may be attributed to the fact that the IPAS has similar tissue structure and properties as the spleen, which possesses the lowest ADC values among the upper abdominal viscera.

Our study had several limitations. First, selection bias may be present due to its retrospective nature. Second, the number of enrolled patients is small. As we know, an IPAS is an uncommon condition, with a prevalence ranging from 1.1%-3.4% in individuals[25]. We could not include more IPAS patients in a short period of time. We will recruit more patients for further validation and reliability testing of our results. Third, although no difference regarding diagnostic performance of absolute ADC and normalized ADC values in discrimination of IPAS from PNET was observed, further studies with a larger cohort size may be needed to evaluate the definite superiority of one method over another. Fourth, there was no histopathological confirmation of IPAS in 6 cases since surgical resection is not recommended for IPAS. However, reasonable confidence was acquired with the criteria for the imaging diagnosis of IPAS combining typical imaging features and stability on imaging follow-up.

CONCLUSION

In conclusion, our study demonstrated that both absolute ADC and normalized ADC values allow clinically relevant differentiation of IPAS from PNET. Large-scale multicenter prospective cohort studies are needed to validate the potential value of absolute and normalized ADC values in differentiating IPAS from PNET.

ARTICLE HIGHLIGHTS

Research background

Intrapancreatic accessory spleen (IPAS) typically presents as a solitary, well-defined, hypervascular, ovoid or round mass with a maximum diameter < 3 cm on contrast-enhanced (CE) computed tomography or CE magnetic resonance imaging. They are often misdiagnosed as small (< 3 cm) hypervascular pancreatic neuroendocrine tumors (PNETs) since they share similar imaging findings. IPAS is innocuous in nature and generally does not require any treatment. However, surgery and/or chemotherapy are recommended for PNETs.

Research motivation

The overlap of imaging features between IPAS and small (< 3 cm) hypervascular PNET often requires surgical management. Therefore, preoperative characterization of IPAS *vs* small (< 3 cm) hypervascular PNET is of utmost importance. This study provided a non-invasive method for preoperatively differentiating these two entities.

Research objectives

This study aimed to investigate and compare the diagnostic performance of absolute apparent diffusion coefficient (ADC) and normalized ADC (lesion-to-spleen ADC ratios) in the differential diagnosis of IPAS from PNET.

Research methods

A retrospective study consisting of 16 PNET patients and 13 IPAS patients who underwent preoperative CE-magnetic resonance imaging together with diffusion-weighted imaging/ADC maps was performed. Two independent reviewers measured ADC on all lesions and spleens, and normalized ADC was calculated for further analysis. The receiver operating characteristics analysis was carried out for evaluating the diagnostic performance of both absolute ADC and normalized ADC values. Inter-reader reliability for the two methods was evaluated.

Research results

IPAS had significantly lower absolute ADC ($0.931 \pm 0.773 \times 10^{-3} \text{ mm}^2/\text{s}$ vs $1.254 \pm 0.219 \times 10^{-3} \text{ mm}^2/\text{s}$) and normalized ADC values (1.154 ± 0.167 vs 1.591 ± 0.364) as compared to PNET. A cutoff value of $1.046 \times 10^{-3} \text{ mm}^2/\text{s}$ for absolute ADC was associated with 81.25% sensitivity, 100% specificity, and 89.66% accuracy with an area under curve of 0.94 for the differential diagnosis of IPAS from PNET. Similarly, a cutoff value of 1.342 for normalized ADC was associated with 81.25% sensitivity, 92.31% specificity, and 86.21% accuracy with an area under the curve of 0.91 for the differential diagnosis of IPAS from PNET. Both methods showed excellent inter-reader reliability with intraclass correlation coefficients for absolute ADC and ADC ratio of 0.968 and 0.976, respectively.

Research conclusions

This study demonstrated that both absolute ADC and normalized ADC values allow clinically relevant differentiation of IPAS from PNET.

Research perspectives

This study provided a non-invasive method to preoperatively differentiate IPAS from PNET, which has a profound clinical significance in guiding treatment strategy and predicting prognosis for patients with IPAS and PNET. Large-scale multicenter prospective cohort studies are needed to validate the potential value of absolute and normalized ADC values in differentiating IPAS from PNET.

ACKNOWLEDGEMENTS

We thank all authors for their continuous and excellent support with patient data collection, imaging analysis, statistical analysis, and valuable suggestions for the article.

FOOTNOTES

Author contributions: Ren S, Guo K, and Li Y contributed equally to this work; Ren S, Wang ZQ, and Tian Y designed the research study; Ren S, Guo K, Li Y, and Cao YY performed the research; Ren S, Guo K, and Li Y analyzed the data; Ren S wrote the manuscript; Wang ZQ and Tian Y revised the manuscript; All authors read and approved the final manuscript.

Supported by the National Natural Science foundation of China, No. 82202135, and No. 82171925; Foundation of Excellent Young Doctor of Jiangsu Province Hospital of Chinese Medicine, No. 2023QB0112; Innovative Development Foundation of Department in Jiangsu Hospital of Chinese Medicine, No. Y2021CX19; and Developing Program for High-level Academic Talent in Jiangsu Hospital of TCM, No. y2021rc03.

Institutional review board statement: The study was reviewed and approved by the ethics committee of Affiliated Hospital of Nanjing University of Chinese Medicine (Approval No. 2017NL-137-05).

Informed consent statement: Informed consent statement was waived due to the retrospective nature of the study.

Conflict-of-interest statement: The authors declare that they have no conflicts of interest.

Data sharing statement: Patient imaging data and histopathology reports contain sensitive patient information and cannot be released publicly due to the legal and ethical restrictions imposed by the institutional ethics committee (Affiliated Hospital of Nanjing University of Chinese Medicine). Data is available upon reasonable request from the following e-mail address: zhongqiuwang@njucm.edu.cn.

Open-Access: This article is an open-access article that was selected by an in-house editor and fully peer-reviewed by external reviewers. It is distributed in accordance with the Creative Commons Attribution NonCommercial (CC BY-NC 4.0) license, which permits others to distribute, remix, adapt, build upon this work non-commercially, and license their derivative works on different terms, provided the original work is properly cited and the use is non-commercial. See: <https://creativecommons.org/licenses/by-nc/4.0/>

Country/Territory of origin: China

ORCID number: Shuai Ren 0000-0003-4902-6298; Kai Guo 0000-0002-7593-2510; Yuan Li 0000-0002-1454-3976; Ying-Ying Cao 0000-0001-9067-6319; Zhong-Qiu Wang 0000-0001-6681-7345; Ying Tian 0000-0002-1525-0614.

S-Editor: Yan JP

L-Editor: Filipodia

P-Editor: Zhang XD

REFERENCES

- 1 **Pandey A**, Pandey P, Ghasabeh MA, Varzaneh FN, Khoshpouri P, Shao N, Pour MZ, Fouladi DF, Hruban RH, O'Broin-Lennon AM, Kamel IR. Accuracy of apparent diffusion coefficient in differentiating pancreatic neuroendocrine tumour from intrapancreatic accessory spleen. *Eur Radiol* 2018; **28**: 1560-1567 [PMID: 29134352 DOI: 10.1007/s00330-017-5122-3]
- 2 **Smith HC**, Kakar N, Shadid AM. Accessory Spleen Masquerading as an Intrapancreatic Tumor: A Case Report. *Cureus* 2022; **14**: e24677 [PMID: 35663712 DOI: 10.7759/cureus.24677]
- 3 **Wong A**, Fung KFK, Wong WC, Ng KK, Kung BT, Kan YLE. Multimodality imaging of developmental splenic anomalies: tips and pitfalls. *Clin Radiol* 2022; **77**: 319-325 [PMID: 35000764 DOI: 10.1016/j.crad.2021.12.014]
- 4 **Bhutiani N**, Egger ME, Doughtie CA, Burkardt ES, Scoggins CR, Martin RC 2nd, McMasters KM. Intrapancreatic accessory spleen (IPAS): A single-institution experience and review of the literature. *Am J Surg* 2017; **213**: 816-820 [PMID: 27894508 DOI: 10.1016/j.amjsurg.2016.11.030]
- 5 **Ishigami K**, Nishie A, Nakayama T, Asayama Y, Kakihara D, Fujita N, Ushijima Y, Okamoto D, Ohtsuka T, Mori Y, Ito T, Mochidome N, Honda H. Superparamagnetic iron-oxide-enhanced diffusion-weighted magnetic resonance imaging for the diagnosis of intrapancreatic accessory spleen. *Abdom Radiol (NY)* 2019; **44**: 3325-3335 [PMID: 31420705 DOI: 10.1007/s00261-019-02189-8]
- 6 **Kang BK**, Kim JH, Byun JH, Lee SS, Kim HJ, Kim SY, Lee MG. Diffusion-weighted MRI: usefulness for differentiating intrapancreatic accessory spleen and small hypervascular neuroendocrine tumor of the pancreas. *Acta Radiol* 2014; **55**: 1157-1165 [PMID: 24259300 DOI: 10.1177/0284185113513760]
- 7 **Jang KM**, Kim SH, Lee SJ, Park MJ, Lee MH, Choi D. Differentiation of an intrapancreatic accessory spleen from a small (<3-cm) solid pancreatic tumor: value of diffusion-weighted MR imaging. *Radiology* 2013; **266**: 159-167 [PMID: 23093681 DOI: 10.1148/radiol.12112765]
- 8 **Lin X**, Xu L, Wu A, Guo C, Chen X, Wang Z. Differentiation of intrapancreatic accessory spleen from small hypervascular neuroendocrine tumor of the pancreas: textural analysis on contrast-enhanced computed tomography. *Acta Radiol* 2019; **60**: 553-560 [PMID: 30086651 DOI: 10.1177/0284185118788895]
- 9 **Yin Q**, Wang M, Wang C, Wu Z, Yuan F, Chen K, Tang Y, Zhao X, Miao F. Differentiation between benign and malignant solid pseudopapillary tumor of the pancreas by MDCT. *Eur J Radiol* 2012; **81**: 3010-3018 [PMID: 22520082 DOI: 10.1016/j.ejrad.2012.03.013]
- 10 **Huang M**, Li J, Yin Q, Xiong L. Surgical Strategy and Prognosis of Pancreatic Neuroendocrine Tumors Based on Smart Medical Imaging. *Contrast Media Mol Imaging* 2022; **2022**: 8752375 [PMID: 35821889 DOI: 10.1155/2022/8752375]
- 11 **Kato T**, Matsuo Y, Ueda G, Aoyama Y, Omi K, Hayashi Y, Imafuji H, Saito K, Tsuboi K, Morimoto M, Ogawa R, Takahashi H, Kato H, Yoshida M, Naitoh I, Hayashi K, Takahashi S, Takiguchi S. Epithelial cyst arising in an intrapancreatic accessory spleen: a case report of robotic surgery and review of minimally invasive treatment. *BMC Surg* 2020; **20**: 263 [PMID: 33129283 DOI: 10.1186/s12893-020-00927-0]
- 12 **Kurita A**, Mori Y, Someya Y, Kubo S, Azuma S, Iwano K, Ikeda S, Okumura R, Yazumi S. High signal intensity on diffusion-weighted magnetic resonance images is a useful finding for detecting early-stage pancreatic cancer. *Abdom Radiol (NY)* 2021; **46**: 4817-4827 [PMID: 34223962 DOI: 10.1007/s00261-021-03199-1]
- 13 **Gong XH**, Xu JR, Qian LJ. Atypical and uncommon CT and MR imaging presentations of pancreatic ductal adenocarcinoma. *Abdom Radiol (NY)* 2021; **46**: 4226-4237 [PMID: 33914139 DOI: 10.1007/s00261-021-03089-6]
- 14 **Jia H**, Li J, Huang W, Lin G. Multimodal magnetic resonance imaging of mass-forming autoimmune pancreatitis: differential diagnosis with pancreatic ductal adenocarcinoma. *BMC Med Imaging* 2021; **21**: 149 [PMID: 34654379 DOI: 10.1186/s12880-021-00679-0]
- 15 **Zeng P**, Ma L, Liu J, Song Z, Yuan H. The diagnostic value of intravoxel incoherent motion diffusion-weighted imaging for distinguishing nonhypervascular pancreatic neuroendocrine tumors from pancreatic ductal adenocarcinomas. *Eur J Radiol* 2022; **150**: 110261 [PMID: 35316674 DOI: 10.1016/j.ejrad.2022.110261]
- 16 **Grech-Sollars M**, Hales PW, Miyazaki K, Raschke F, Rodriguez D, Wilson M, Gill SK, Banks T, Saunders DE, Clayden JD, Gwilliam MN, Barrick TR, Morgan PS, Davies NP, Rössler J, Auer DP, Grundy R, Leach MO, Howe FA, Peet AC, Clark CA. Multi-centre reproducibility of diffusion MRI parameters for clinical sequences in the brain. *NMR Biomed* 2015; **28**: 468-485 [PMID: 25802212 DOI: 10.1002/nbm.3269]
- 17 **Ye XH**, Gao JY, Yang ZH, Liu Y. Apparent diffusion coefficient reproducibility of the pancreas measured at different MR scanners using diffusion-weighted imaging. *J Magn Reson Imaging* 2014; **40**: 1375-1381 [PMID: 24222019 DOI: 10.1002/jmri.24492]
- 18 **Jang W**, Song JS, Kwak HS, Hwang SB, Paek MY. Intra-individual comparison of conventional and simultaneous multislice-accelerated diffusion-weighted imaging in upper abdominal solid organs: value of ADC normalization using the spleen as a reference organ. *Abdom Radiol (NY)* 2019; **44**: 1808-1815 [PMID: 30737546 DOI: 10.1007/s00261-019-01924-5]
- 19 **Ding X**, Xu H, Zhou J, Xu J, Mei H, Long Q, Wang Y. Reproducibility of normalized apparent diffusion coefficient measurements on 3.0-T diffusion-weighted imaging of normal pancreas in a healthy population. *Medicine (Baltimore)* 2019; **98**: e15104 [PMID: 30946375 DOI: 10.1097/MD.00000000000015104]
- 20 **Guo CG**, Ren S, Chen X, Wang QD, Xiao WB, Zhang JF, Duan SF, Wang ZQ. Pancreatic neuroendocrine tumor: prediction of the tumor grade using magnetic resonance imaging findings and texture analysis with 3-T magnetic resonance. *Cancer Manag Res* 2019; **11**: 1933-1944 [PMID: 30881119 DOI: 10.2147/CMAR.S195376]
- 21 **Ma C**, Yang P, Li J, Bian Y, Wang L, Lu J. Pancreatic adenocarcinoma: variability in measurements of tumor size among computed tomography, magnetic resonance imaging, and pathologic specimens. *Abdom Radiol (NY)* 2020; **45**: 782-788 [PMID: 31292672 DOI: 10.1007/s00261-019-02125-w]
- 22 **Vandekerckhove E**, Ameloot E, Hoorens A, De Man K, Berrevoet F, Geboes K. Intrapancreatic accessory spleen mimicking pancreatic NET: can unnecessary surgery be avoided? *Acta Clin Belg* 2021; **76**: 492-495 [PMID: 32394810 DOI: 10.1080/17843286.2020.1762351]

- 23 **Kim SH**, Lee JM, Han JK, Lee JY, Kang WJ, Jang JY, Shin KS, Cho KC, Choi BI. MDCT and superparamagnetic iron oxide (SPIO)-enhanced MR findings of intrapancreatic accessory spleen in seven patients. *Eur Radiol* 2006; **16**: 1887-1897 [PMID: 16547707 DOI: 10.1007/s00330-006-0193-6]
- 24 **Kim SH**, Lee JM, Han JK, Lee JY, Kim KW, Cho KC, Choi BI. Intrapancreatic accessory spleen: findings on MR Imaging, CT, US and scintigraphy, and the pathologic analysis. *Korean J Radiol* 2008; **9**: 162-174 [PMID: 18385564 DOI: 10.3348/kjr.2008.9.2.162]
- 25 **Li BQ**, Xu XQ, Guo JC. Intrapancreatic accessory spleen: a diagnostic dilemma. *HPB (Oxford)* 2018; **20**: 1004-1011 [PMID: 29843985 DOI: 10.1016/j.hpb.2018.04.004]



Published by **Baishideng Publishing Group Inc**
7041 Koll Center Parkway, Suite 160, Pleasanton, CA 94566, USA
Telephone: +1-925-3991568
E-mail: bpgoffice@wjgnet.com
Help Desk: <https://www.f6publishing.com/helpdesk>
<https://www.wjgnet.com>

